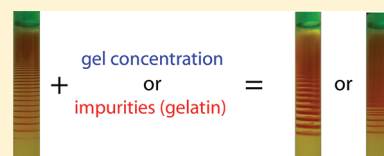


Controlling and Engineering Precipitation Patterns

István Lagzi^{*,†,‡}[†]Department of Physics, Budapest University of Technology and Economics, H-1111 Budapest, Budafoki út 8, Hungary[‡]Department of Meteorology, Eötvös Loránd University, Budapest, Hungary

ABSTRACT: Controlling and engineering chemical structures are the most important scientific challenges in material science. Precipitation patterns from ions or nanoparticles are promising candidates for designing bulk structure for catalysis, energy production, storage, and electronics. There are only a few procedures and techniques to control precipitation (Liesegang) patterns in gel media (e.g., using an electric field, varying the initial concentration of the electrolytes). However, those methods provide just a limited

degree of freedom. Here, we provide a robust and transparent way to control and engineer Liesegang patterns by varying gel concentration and inducing impurity by addition of gelatin to agarose gel. Using this experimental method, different precipitation structures can be obtained with different width and spatial distribution of the formed bands. A new variant of a sol-coagulation model was developed to describe and understand the effect of the gel concentration and impurities on Liesegang pattern formation.



INTRODUCTION

Self-organization and self-assembly of components at atomic, molecular, and nanoscopic levels have gained growing interest in the past decades due to their importance in material science.^{1,2} Understanding governing forces and interactions between building blocks at small scales is a key element in designing new materials for useful applications (e.g., catalysis, energy storage and production, medicine).³ One of the spontaneous pattern formations is the periodic precipitation (Liesegang phenomenon), where distinct zones form periodically in space and time due to the diffusion of two coprecipitating chemical species and their precipitation reaction.⁴ Recently, there has been a resurgent interest in this reaction-diffusion phenomenon because of its applications in bottom-up fabrication.⁵ Controlling precipitation structures is among the most challenging problems because of the ionic nature of chemical species⁶ and their interaction with the gel structure.^{7,8} An obvious choice to control such structure is applying an electric field to modify the mass transport of charged chemical species, thus altering the diffusive transport nature of ions and having a dramatic effect on pattern formation.^{6,9–12}

Liesegang patterns have several regularities, which can describe and characterize the spatiotemporal pattern formation. Distance between bands in regular Liesegang phenomenon is nonequidistant (distances of the bands from the gel interface increase according to a geometrical series).¹³ The structure can be characterized by the so-called spacing coefficient ($p = (x_{n+1} - x_n)/(x_n)$, where x_{n+1} and x_n are the position of two consecutive bands measured from the junction point of the electrolytes). This is the so-called spacing law.¹³ It has been found experimentally that the spacing coefficient depends on the initial concentrations a_0 and b_0 of the outer and inner

electrolytes, and this can be described by the following relation (Matalon-Packter law):¹⁴

$$p = f(b_0) + \frac{g(b_0)}{a_0} \quad (1)$$

where f and g are the decreasing functions in their arguments. This regularity provides a simple but not flexible way to control Liesegang patterns via changing initial concentration of the electrolytes.

Interestingly, recent works have shown that precipitation patterns can emerge not only in precipitating inorganic salt (ionic) systems, but in systems containing oppositely charged noble metal nanoparticles quantum dots (CdS) stabilized by thiol groups.^{15–17}

In the usual experimental setup of precipitation pattern formation (Liesegang phenomenon), one electrolyte (the so-called inner electrolyte) is homogeneously distributed in a gel, while another (outer electrolyte) diffuses into the gel from the specific reservoir. In the simplest case, the outer electrolyte is poured on top of a gel column in a test tube. After some time, depending on the geometry of the system or its chemical composition and gel structure, variety of the pattern can be observed including regular band formation,^{4,18} invert type Liesegang banding,^{19,20} dendrites having fractal structure,^{21,22} and dynamic precipitation waves.²³ All reaction-diffusion models developed to describe pattern formation in gelled media are based on calculating diffusion of species and their precipitation reaction neglecting the effect of the gel on these phenomena.^{24–30} There are several recent experimental works, which emphasize the importance of the supporting media in pattern formation.^{7,31–33} In some cases changing the chemical

Received: December 13, 2011

Revised: January 16, 2012

Published: January 30, 2012

property of the gel can result in quite different precipitation phenomena, for instance, replacing gelatin in $\text{Ag}_2\text{Cr}_2\text{O}_7$ system to agarose can give rise to a crossover from regular Liesegang pattern formation to a tree-like precipitation pattern.⁷

In this paper, we will provide an alternative way to control and design regular precipitation (Liesegang) patterns via varying experimental conditions like gel concentration and the chemical composition (purity) of the gel. Gel concentration affects the pore size of the gel, thus limiting the density of the precipitate, and chemical impurities in the gel can lower the precipitation threshold. A modified sol-coagulation model was developed to take into account these effects, and this model is able to explain the experimentally observed results.

EXPERIMENTAL SECTION

An agarose gel containing potassium chromate as inner electrolyte was prepared as follows. A sample of potassium chromate (K_2CrO_4 , Sigma-Aldrich) was dissolved in double-distilled water with the given amount of agarose powder (Type I, Sigma-Aldrich). The mixture was heated to 90 °C under constant stirring until a homogeneous solution was obtained. The resulting solution was then poured into a set of test tubes of 16 mm diameter, then the solution was left for 2 h at 5.7 °C. After polymerization a solution of copper chloride (CuCl_2 , Sigma-Aldrich) was gently poured on top of the potassium chromate-doped gel. The tubes were then covered and left in a thermostat at 5.7 ± 0.3 °C. The pattern formation according to the chemical reaction $\text{Cu}^{2+}(\text{aq}) + \text{CrO}_4^{2-}(\text{aq}) \rightarrow \text{CuCrO}_4(\text{s})$ was monitored by a digital camera for 7 days.

MODELING

A simple chemical mechanism to produce precipitate consists of two reaction steps incorporating an intermediate species. This mechanism can be written as



where A and B are the outer and inner electrolytes, and C is the intermediate product (sol), which can transform to precipitate (D). Usually the initial condition is such that the concentration of the outer electrolyte (A) is much higher than that of the inner electrolyte (B); thus, the pattern formation is governed by the diffusion front of the outer electrolyte. In the sol-coagulation model, C forms continuously behind the chemical front, and this can turn to immobile precipitate D, if the local concentration of C reaches a coagulation threshold.³⁴ Moreover, the precipitate can grow further by an autocatalytic process, which depletes the intermediate species in the vicinity of the formed precipitation zone. This process is much faster than the diffusion of chemical species; therefore, this is responsible for distinct band formation. These processes can be written in a set of partial differential equations, which describes the spatiotemporal evolution of the pattern

$$\partial_t a = D_a \nabla^2 a - kab \quad (4)$$

$$\partial_t b = D_b \nabla^2 b - kab \quad (5)$$

$$\partial_t c = D_c \nabla^2 c + kab - \kappa_1 c \Theta(c - c^*) - \kappa_2 cd \quad (6)$$

$$\partial_t d = \kappa_1 c \Theta(c - c^*) + \kappa_2 cd \quad (7)$$

Here a , b , and c are the concentrations of A, B, and C respectively, while d is the density (concentration) of the precipitate. D_a , D_b , and D_c are the diffusion coefficients of the

corresponding species. k is the chemical rate constant for reaction 2, and κ_1 and κ_2 are the rate constants for the coagulation and the autocatalytic precipitate formation, respectively. Θ denotes the Heaviside step function. The main problem of this model is that it does not reproduce the finite widths of the precipitation bands (Figure 1a) and the

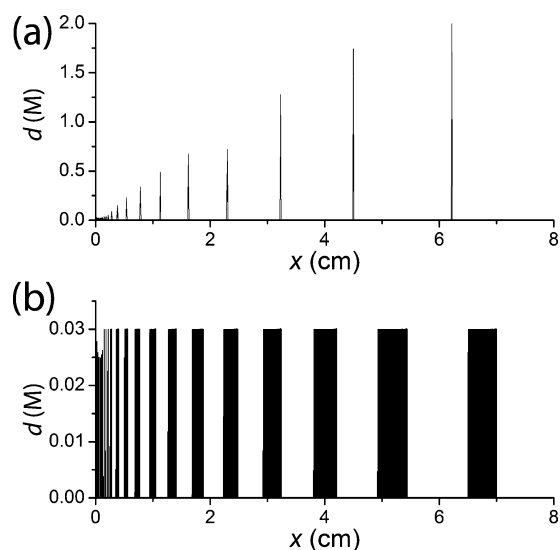


Figure 1. Results of the numerical simulations of regular (Liesegang) patterns in 1D using a standard sol-coagulation model with $\rho \rightarrow \infty$ (there is no limitation of the maximal amount of precipitate) (a) and an extended sol-coagulation model used in this study with $\rho = 0.03$ M (b). The following parameter set was used: $D_a = D_b = D_c = 10^{-9}$ m² s, $k = 1$ M⁻¹ s⁻¹, $\kappa_1 = 1$ s⁻¹, $\kappa_2 = 1$ M⁻¹ s⁻¹, $c^* = 6 \times 10^{-3}$ M, $a_0 = 0.5$ M, $b_0 = 0.01$ M. The time step and the grid size were 1 s and 10^{-4} m, respectively.

model results in patterns comprising disjoint precipitation spots/dots rather than continuous zones in case of radial diffusion in 2D, which is due to the fast autocatalytic precipitate growth. In original sol-coagulation models, there is no limit for precipitate formation at a given spatial position, and it is responsible for this behavior, which is definitely an artifact of the model. Therefore, this sol-coagulation scenario was extended further to overcome this problem. We introduce a new parameter in the model—the maximal amount of precipitate (ρ) which can be formed. In other words, we limited the maximal amount of the formed precipitate. If the total amount of the precipitate reaches this ρ , no further growth occurs at the given spatial position, and there will be no coagulation threshold at the neighboring positions. Mathematically, this assumption can be written as

$$\begin{aligned} \text{if } c(t, x_n) < \rho \text{ then } \kappa_1(t, x_n) &= \kappa_1, \\ \kappa_2(t, x_n) &= \kappa_2 \text{ and} \\ c^*(t, x_{n-1}) &= c^*(t, x_{n+1}) = c^* \end{aligned} \quad (8)$$

$$\begin{aligned} \text{if } c(t, x_n) \geq \rho \text{ then } \kappa_1(t, x_n) &= \kappa_2(t, x_n) = 0 \\ \text{and } c^*(t, x_{n-1}) &= c^*(t, x_{n+1}) = 0 \end{aligned} \quad (9)$$

where $\kappa_1(t, x_{n-1})$, $\kappa_2(t, x_{n+1})$, and $c^*(t, x_{n-1})$, $c^*(t, x_{n+1})$ are the chemical rate constants for precipitation and the coagulation threshold at the neighboring positions (grid cells/points).

Regular Liesegang bands with increasing widths can be reproduced using this extension (Figure 1b).

Reaction-diffusion eqs 4–7 were solved using a standard “method of lines” technique. Spatially a standard finite-difference method on a 1D equidistant grid was applied followed by time integration (backward Euler method) to solve the resulting ordinary differential equations with the following initial conditions: $a(t = 0, x) = 0$, $b(t = 0, x) = b_0$, $c(t = 0, x) = 0$, $d(t = 0, x) = 0$. No-flux boundary conditions were applied for all chemical species at both ends of the domain except for A (outer electrolyte), where a Dirichlet boundary condition ($a|_{x=0} = a_0$) was used at $x = 0$ position (junction point of the electrolytes), where a_0 is the initial concentration of the outer electrolyte.

RESULTS AND DISCUSSION

Investigating the effect of the supporting (gelled) media on pattern formation is a key element for understanding the involved pattern formation phenomena. In precipitation systems, the usual argument is that the gel just prevents sedimentation and hydrodynamic instability. However, former and recent works show transparently that gel can have a sometimes dramatic effect on pattern formation.^{7,8} On the other hand, understanding “gel–precipitate” interaction could help to provide new methods and techniques to design bulk precipitation structures.

We investigated the effect of gel concentration on Liesegang pattern formation (Figure 2a). Increasing the gel concentration produces bands with increasing spacing coefficient and decreasing bandwidth. This finding has two important aspects. First, changing gel concentration involves changes in spacing coefficient of the pattern (Figure 3a), which demonstrates that the Matalon-Packter law¹⁴ (eq 1) is a nonuniversal regularity, and that the spacing coefficient depends not only on initial concentration of the electrolytes, but also on the gel concentration. This also raises questions regarding the mechanism of nucleation, precipitate growth, and ripening. The second aspect is the width of the formed bands. It is a usual statement in Liesegang systems that the width of the bands (w_n) is linearly proportional to their positions (x_n), i.e., $x_n \sim w_n$.²⁷ This relationship (width law) is a direct consequence of the mass conservation and the assumptions that the reaction front leaves behind a constant density (c_0) of the intermediate product (C), and this intermediate product can segregate into low (c_l) and high (c_h) density bands.^{27,28} Combining these three assumptions together with the spacing law ($p = (x_{n+1} - x_n)/(x_n)$) gives the following relationship

$$w_n = \frac{p(c_0 - c_l)}{(c_h - c_l)} x_n \quad (8)$$

which is the so-called width law.³⁵ This law predicts that the 2-fold increase in the position of the bands measured from the junction point of the electrolytes should result in a 2-fold increase in the width of the bands. However, it is vividly seen that the regular Liesegang patterns do not fulfill this regularity (Figures 2a and 4a). The widths of the precipitation bands do not change much (at least not linearly) with their position, which indicates that the maximal amount of precipitate which can be formed at the given position (ρ) is higher than c_h ($\rho \gg c_h$). Agarose gel has a relatively large pore size compared to other gels, and that is why agarose gel is the most popular and suitable for gel electrophoresis, where even big macromolecules

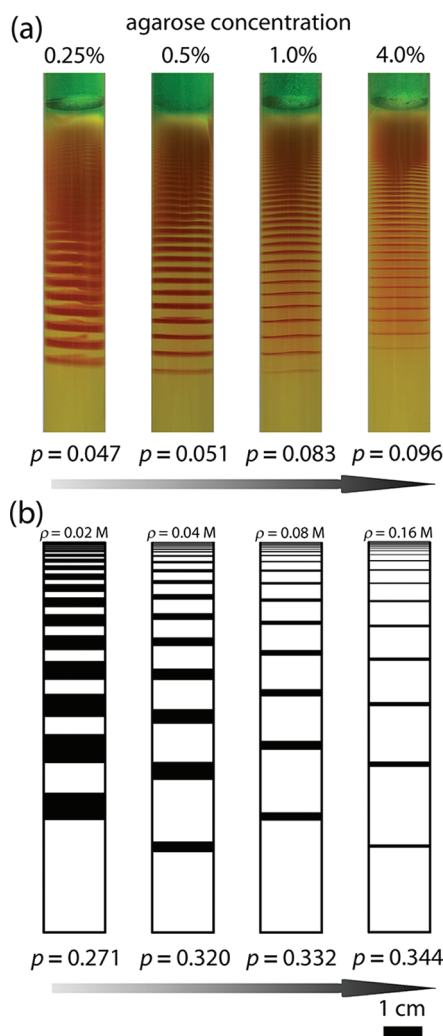


Figure 2. Controlling Liesegang patterns with the agarose gel concentration (a). The concentration of copper chloride (outer electrolyte) and potassium chromate (inner electrolyte) was 0.5 and 0.01 M, respectively. Results of the numerical simulations using an extended sol-coagulation model (b): $D_a = D_b = D_c = 10^{-9} \text{ m}^2 \text{ s}$, $k = 1 \text{ M}^{-1} \text{ s}^{-1}$, $\kappa_1 = 1 \text{ s}^{-1}$, $\kappa_2 = 1 \text{ M}^{-1} \text{ s}^{-1}$, $c^* = 6 \times 10^{-3} \text{ M}$, $a_0 = 0.5 \text{ M}$, $b_0 = 0.01 \text{ M}$. The maximal amount of precipitate (ρ) was varied between 0.02 and 0.16 M as a consequence of the agarose gel concentration.

can migrate through a gel sheet. The average pore size in a 0.5% gel is 550 nm and in a 4% gel is 250 nm, respectively.³⁶ This indicates that bigger colloid particles can easily diffuse even in a hard ($\sim 4\%$) agarose gel. This can result in no significant difference in the velocity of chemical fronts in soft and hard gels. Experimental observations support this argument; there were no differences in front velocities. On the other hand, harder gel has bigger internal gel surfaces, which play an important role in heterogeneous nucleation and precipitate growth. Higher surface area can “trap” more precipitate, which can be translated into the mathematical model with higher maximal amount of precipitate (ρ). Using this assumption that the soft gel has lower maximal amount of precipitate than the harder gel can reproduce all features observed in experiments, namely, the variation of the width of the bands and the corresponding spacing coefficients (Figure 2b). Increasing the gel concentration (increasing the maximal amount of precipitate in the model) produces bands with increasing

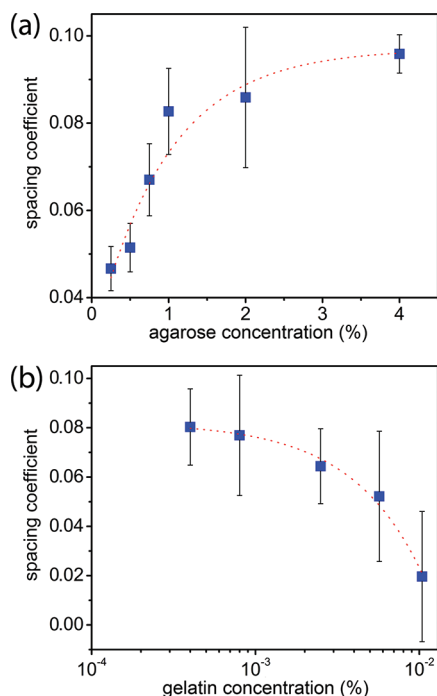


Figure 3. Variation of the spacing coefficient changing the agarose gel concentration (a) and the gelatin concentration in a 1% agarose gel (b). The concentration of copper chloride (outer electrolyte) and potassium chromate (inner electrolyte) was 0.5 and 0.01 M, respectively.

spatial coefficient and decreasing bandwidth similar to the experimental results.

The second interesting aspect of the control and engineering of precipitation patterns is the variation of the purity of the supporting medium. There are a few experimental papers regarding the effect of the gel impurity on pattern structure.^{7,37} The consequences of impurities have also been considered in theoretical work using a lattice-gas simulation.³⁷ Recently, we showed that addition of a small amount of gelatin ($10^{-3}\%$) to agarose can enhance the formation of Liesegang banding, while in a pure agarose gel (no gelatin added) no Liesegang pattern formation was observed in the $\text{Ag}_2\text{Cr}_2\text{O}_7$ system.

A small amount of gelatin (between $4 \times 10^{-4}\%$ and $5 \times 10^{-2}\%$) was added during the gel preparation to the agarose gel (1%) to investigate the effect of impurity of the gel on pattern structure. An increase of the amount of gelatin in agarose gel can produce Liesegang patterns with decreasing spacing coefficient and increasing thickness of the continuous precipitation zone at the gel interface (Figures 3b and 4a). Moreover, at relatively high gelatin concentration ($5 \times 10^{-2}\%$) a continuous precipitation zone forms, thus showing a crossover from regular precipitation pattern to a continuous precipitation band. This can be explained by the fact that the small amount of gelatin in agarose can induce heterogeneous nucleation. By increasing the gelatin concentration in the mixed gel, the heterogeneous nucleation rate and the number density of colloids (intermediate species) will be high enough to produce regular Liesegang patterns with decreasing spacing coefficient. At higher gelatin concentration, continuous precipitation can be observed due to high nucleation/coagulation rate. In the model this effect can be implemented by varying the coagulation threshold (c^*), since higher gelatin (impurity) concentration in agarose gel can result in a lower

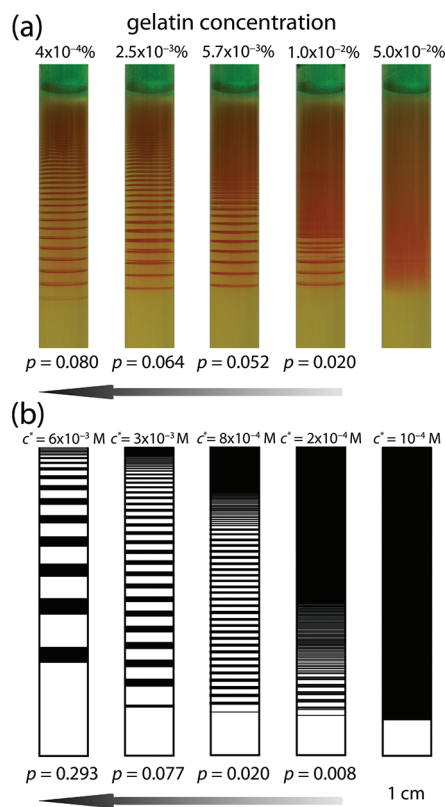


Figure 4. Controlling Liesegang patterns with the addition of gelatin to a 1% agarose gel (a). The concentration of copper chloride (outer electrolyte) and potassium chromate (inner electrolyte) was 0.5 and 0.01 M, respectively. Results of the numerical simulations using an extended sol-coagulation model (b): $D_a = D_b = D_c = 10^{-9} \text{ m}^2 \text{ s}$, $k = 1 \text{ M}^{-1} \text{ s}^{-1}$, $\kappa_1 = 1 \text{ s}^{-1}$, $\kappa_2 = 1 \text{ M}^{-1} \text{ s}^{-1}$, $\rho = 0.03 \text{ M}$, $a_0 = 0.5 \text{ M}$, $b_0 = 0.01 \text{ M}$. The coagulation threshold (c^*) was varied between 10^{-4} M and 6×10^{-3} M as a consequence of the presence of gelatin (impurity) in agarose gel.

coagulation threshold (Figure 4b). After implementing this extension, the numerical model is able to reproduce all features observed in the experiments (Figure 4).

CONCLUSIONS

In summary, we show a robust way to control and engineer precipitation structures through the variation of the gel concentration/strength and inducing some “chemical” perturbation to the system by adding impurities (gelatin) to the agarose gel. Our experimental results provide a new chemical way to control Liesegang patterns, which can be useful for engineering special heterogeneous catalysts or bulk precipitation structures. We can easily control the structure of the Liesegang patterns through the width of the formed bands and the spacing coefficient of the pattern. Combining these two independent methods can provide a rich variety of possible patterns. To support our experimental observations, a new variant of the sol-coagulation model was developed introducing a new quantity, the maximal amount of precipitate (ρ). By varying this quantity and the coagulation threshold, we were able to describe and understand the observed trends in experiments. In such a way, we could indirectly incorporate the effect of the gel on pattern formation in a model. This will allow us to introduce new methods to chemically design and control precipitation patterns.

AUTHOR INFORMATION

Corresponding Author

*E-mail: lagzi@vuk.chem.elte.hu, Tel.:+361-463-1341, Fax:+361-463-4180.

Notes

The authors declare no competing financial interest.

ACKNOWLEDGMENTS

Authors acknowledge the financial support of the Hungarian Research Found (OTKA K81933 and K77908) and the European Union and the European Social Fund (TÁMOP 4.2.1./B-09/KMR-2010-0003).

REFERENCES

- (1) Whitesides, G. M.; Grzybowski, B. *Science* **2002**, *295*, 2418–2421.
- (2) Whitesides, G. M.; Boncheva, M. *Proc. Natl. Acad. Sci. U.S.A.* **2002**, *99*, 4769–4774.
- (3) Bishop, K. J. M.; Wilmer, C. E.; Soh, S.; Grzybowski, B. A. *Small* **2009**, *5*, 1600–1630.
- (4) Sadek, S.; Sultan, R. In *Precipitation Patterns in Reaction-Diffusion Systems*, Lagzi, I. Ed.; Research Signpost: Trivandrum, 2010; p 1.
- (5) Yan, H.; Zhao, Y.; Qiu, C.; Wu, H. *Sens. Actuators, B* **2008**, *132*, 20–25.
- (6) Bena, I.; Droz, M.; Lagzi, I.; Martens, K.; Rácz, Z.; Volford, A. *Phys. Rev. Lett.* **2008**, *101*, 075701.
- (7) Lagzi, I.; Ueyama, D. *Chem. Phys. Lett.* **2009**, *468*, 188–192.
- (8) Toramaru, A.; Harada, T.; Okamura, T. *Physica D* **2003**, *183*, 133–140.
- (9) Makki, R.; Al-Ghoul, M.; Sultan, R. *J. Phys. Chem. A* **2009**, *113*, 6049–6057.
- (10) Lagzi, I. *Phys. Chem. Chem. Phys.* **2002**, *4*, 1268–1270.
- (11) Al-Ghoul, M.; Sultan, R. *J. Phys. Chem. A* **2009**, *107*, 1095–1101.
- (12) Bena, I.; Droz, M.; Rácz, Z. *J. Chem. Phys.* **2005**, *122*, 204502.
- (13) Jablczynski, C. K. *Bull. Soc. Chim. France* **1923**, *33*, 1592–1602.
- (14) Matalon, R.; Packter, A. *J. Colloid. Sci.* **1955**, *10*, 46–62.
- (15) Lagzi, I.; Bartłomiej, K.; Grzybowski, B. A. *J. Am. Chem. Soc.* **2010**, *132*, 58–59.
- (16) Al-Ghoul, M.; Ghaddar, T.; Moukalled, T. *J. Phys. Chem. B* **2009**, *113*, 11594–11603.
- (17) Al-Ghoul, M.; Ghaddar, T. *J. Nano Res.* **2010**, *11*, 19–24.
- (18) Narita, T.; Tokita, M. *Langmuir* **2006**, *22*, 349–352.
- (19) Karam, T.; El-Rassy, H.; Sultan, R. *J. Phys. Chem. A* **2011**, *115*, 2994–2998.
- (20) Molnár, F.; Izsák, F.; I. Lagzi, I. *Phys. Chem. Chem. Phys.* **2008**, *10*, 2368–2373.
- (21) Mandalian, L.; Sultan, R. *Collect. Czech. Chem. C* **2002**, *67*, 1729–1742.
- (22) Yin, W. X.; Liu, Y. F.; Zhao, Y.; Bai, S. Y.; Zhu, W. W.; Weng, S. F.; Gao, Q. Y.; Wu, J. G. *Spectrosc. Spect. Anal.* **2009**, *29*, 3101–3105.
- (23) Volford, A.; Izsák, F.; Ripszám, M.; Lagzi, I. *Langmuir* **2007**, *23*, 961–964.
- (24) Keller, J. B.; Rubinow, S. I. *J. Chem. Phys.* **1981**, *74*, 5000–5007.
- (25) Feeney, R.; Schmidt, S. L.; Strickholm, P.; Chadam, J.; Ortoleva, P. *J. Chem. Phys.* **1983**, *78*, 1293–1311.
- (26) Chernavskii, D. S.; Polezhaev, A. A.; Müller, S. C. *Physica D* **1991**, *54*, 160–170.
- (27) Rácz, Z. *Physica A* **1999**, *274*, 50–59.
- (28) Antal, T.; Droz, M.; Magnin, J.; Rácz, Z. *Phys. Rev. Lett.* **1999**, *83*, 2880–2883.
- (29) L'Heureux, I. *Phys. Lett. A* **2008**, *372*, 3001–3009.
- (30) Jahnke, L.; Kantelhardt, J. W. *Eur. Phys. J. ST* **2008**, *161*, 121–141.
- (31) Barge, L. M.; Hammond, D. E.; Chan, M. A.; Potter, S.; Petruska, J.; Neelson, K. H. *Geofluids* **2011**, *11*, 124–133.
- (32) Barge, L. M.; Neelson, K. H.; Petruska, J. *Chem. Phys. Lett.* **2011**, *493*, 340–345.
- (33) Zaknoun, F.; Mokalled, T.; Hariri, A.; Sultan, R. In *Precipitation Patterns in Reaction-Diffusion Systems*, Lagzi, I., Ed.; Research Signpost: Trivandrum, 2010; p 219.
- (34) Antal, T.; Droz, M.; Magnin, J.; Rácz, Z.; Zrínyi, M. *J. Chem. Phys.* **1998**, *109*, 9479–9486.
- (35) Pillai, K. M.; Vaidyan, V. K.; Ittyachan, M. A. *Colloid Polym. Sci.* **1980**, *258*, 831–838.
- (36) Maaloum, M.; Pernodet, N.; Tinland, B. *Electrophoresis* **1998**, *19*, 1606–1610.
- (37) Hillson, P. J. *Trans. Faraday Soc.* **1961**, *57*, 1031–1034.
- (38) Jahnke, L.; Kantelhardt, J. W. *EPL-Europhys. Lett.* **2008**, *84*, 48006.